Mean-field electron-vibrational theory of collective effects in photonic organic materials. Long-range Frenkel exciton polaritons in nanofibers of organic dye

B. D. Fainberg

Citation: AIP Advances **8**, 075314 (2018); doi: 10.1063/1.5030683
View online: https://doi.org/10.1063/1.5030683
View Table of Contents: http://aip.scitation.org/toc/adv/8/7
Published by the American Institute of Physics

Mean-field electron-vibrational theory of collective effects in photonic organic materials. Long-range Frenkel exciton polaritons in nanofibers of organic dye

B. D. Fainberg[a]
Faculty of Sciences, Holon Institute of Technology, 52 Golomb St., Holon 58102, Israel and School of Chemistry, Tel-Aviv University, Tel-Aviv 69978, Israel

(Received 24 March 2018; accepted 3 July 2018; published online 13 July 2018)

We develop a mean-field electron-vibrational theory of light-induced optical properties of photonic organic materials taking the collective effects into account. The theory contains experimentally measured quantities that make it closely related to experiment, and provides a possibility of generalization to a nonlinear regime. Between other things, we explain the additional red shift of the H-aggregate absorption spectra (that are blue-shifted as a whole). We apply the theory to experiment on fraction of a millimeter propagation of Frenkel exciton polaritons in photoexcited organic nanofibers made of thiacyanine dye. A good agreement between theory and experiment is obtained. https://doi.org/10.1063/1.5030683

I. INTRODUCTION

Recently Noginov et al. demonstrated that purely organic materials characterized by low losses with negative dielectric permittivities can be easily fabricated.[1] Specifically, the substantially strong negative dielectric permittivity demonstrated in zinc tetraphenylporphyrin (ZnTPP), suggests that this dye compound can function as a "plasmonic" material. The experimental demonstration of a surface polariton propagating at the ZnTPP/air interface has been realized.[1] Gentile et al.[2] showed that polymer films doped with J-aggregated (TDBC) molecules might exhibit a negative real permittivity in the vicinity of the exciton resonance. Thin films of such material may support surface exciton polariton (EP) modes, in much the same way that thin metal films support surface plasmon-polariton modes. Furthermore, they used the material parameters derived from experiment to demonstrate that nanostructured excitonic materials may support localized surface EP modes. And even the dramatic laser-induced change of the dielectric permittivity of dyes may be realized[3] that can enable us to control the propagation of EP modes.

In addition, organic dye nanofibers demonstrated long-range Frenkel EP propagation at room temperature.[4,5] The long-range Frenkel EPs are formed in organic dye nanofibers at room temperatures owing to a considerably larger oscillator strength compared to inorganic semiconductors.[4] To realize such long-range propagation, the Frenkel EPs should be stable. Their stability is governed by splitting between two branches of the polariton dispersion, the correct calculation of which is of decisive importance. However, this splitting is of the same order of magnitude as the bandwidth of the exciton line. This necessitates the proper description of the Frenkel exciton line shape that is impossible without taking the electron-vibrational interaction into account (especially for H-aggregates, as it took place in experiment[4]). In other words, we needs in an EP theory that takes electron-vibrational interaction into account in a simple way and provides a possibility of generalization to a nonlinear regime.

In this work we develop a mean-field electron-vibrational theory of Frenkel EPs in organic dye structures and apply it to experiment.[4] Our consideration is based on the model of the interaction

[a]Email: fainberg@hit.ac.il

of strong shaped laser pulse with organic molecules, Refs. 6–8, extended to the dipole-dipole intermolecular interactions in the condensed matter. These latters results in two options. The first option correctly describes the behaviour of the first moment of molecular spectra in condensed matter, and specifically, the red shift, according to the Clausius-Mossotti Lorentz-Lorentz (CMLL) mechanism.[9] The second option is related to the dramatic modification of molecular spectra in condensed matter due to aggregation of molecules into J- or H-aggregates. The theory contains experimentally measured quantities that makes it closely related to experiment. Between other things, using the first option, we explain the additional red shift of the H-aggregate experimental absorption spectra[10] (that are blue-shifted as a whole, and the lineshape of which is described by the second option).

The paper is organized as follows. We start with the derivation of equations taking dipole-dipole intermolecular interactions in condensed matter into account. Then we describe the absorption of H-aggregates, Section III, where we show that only taking both options of our mean-field theory into account can explain the experimental results. In Section IV we apply the theory to experiment,[4] and in Section V, we briefly conclude.

II. DERIVATION OF EQUATIONS FOR DIPOLE-DIPOLE INTERMOLECULAR INTERACTIONS IN CONDENSED MATTER

In this section we shall extend equations for vibrationally non-equilibrium populations of molecular electronic states of Refs. 6–8 to a condensed matter. In this picture we considered a molecule with two electronic states $n = 1$ (ground) and 2 (excited) in a solvent described by the Hamiltonian

$$H_0 = \sum_{n=1}^{2} |n\rangle [E_n + W_n(\mathbf{Q})] \langle n| \tag{1}$$

where $E_2 > E_1$, E_n is the energy of state n, $W_n(\mathbf{Q})$ is the adiabatic Hamiltonian of reservoir R (the vibrational subsystems of a molecule and a solvent interacting with the two-level electron system under consideration in state n). The molecule is affected by electromagnetic field $\mathbf{E}(t)$

$$\mathbf{E}(t) = \frac{1}{2}\mathbf{e}\mathcal{E}(t)\exp(-i\omega t) + \text{c.c.} \tag{2}$$

the frequency of which is close to that of the transition $1 \to 2$. Here $\mathcal{E}(t)$ describes the change of the pulse amplitude in time, $\mathbf{e}$ is unit polarization vector.

Since an absorption spectrum of a large molecule in condensed matter consists from overlapping vibronic transitions, we shall single out the contribution from the low frequency (LF) optically active (OA) vibrations $\{\omega_s\}$ to $W_n(\mathbf{Q})$: $W_n(\mathbf{Q}) = W_{nM} + W_{ns}$ where W_{ns} is the sum of the Hamiltonian governing the nuclear degrees of freedom of the solvent in the absence of the solute and LFOA intramolecular vibrations, and the part which describes interactions between the solute and the nuclear degrees of freedom of the solvent; W_{nM} is the Hamiltonian representing the nuclear degrees of freedom of the high frequency (HF) OA vibrations of the solute molecule.

The influence of the vibrational subsystems of a molecule and a solvent on the electronic transition within the range of definite vibronic transition related to HFOA vibration ($\approx 1000 - 1500 cm^{-1}$) can be described as a modulation of this transition by LFOA vibrations $\{\omega_s\}$.[11] We suppose that $\hbar\omega_s \ll k_B T$. Thus $\{\omega_s\}$ is an almost classical system. In accordance with the Franck-Condon principle, an optical electronic transition takes place at a fixed nuclear configuration. Therefore, the quantity $u_{1s}(\mathbf{Q}) = W_{2s}(\mathbf{Q}) - W_{1s}(\mathbf{Q}) - \langle W_{2s}(\mathbf{Q}) - W_{1s}(\mathbf{Q})\rangle_1$ representing electron-vibration coupling is the disturbance of nuclear motion under electronic transition where $\langle\rangle_n$ stands for the trace operation over the reservoir variables in the electronic state n. Electronic transition relaxation stimulated by LFOA vibrations is described by the correlation function $K(t) = \langle\alpha(0)\alpha(t)\rangle$ of the corresponding vibrational disturbance with characteristic attenuation time τ_s[12–14] where $\alpha \equiv -u_{1s}/\hbar$. The analytic solution of the problem under consideration has been obtained due to the presence of a small parameter. For broad vibronic spectra satisfying the "slow modulation" limit, we have $\sigma_{2s}\tau_s^2 \gg 1$ where $\sigma_{2s} = K(0)$ is the LFOA vibration contribution to a second central moment of an absorption spectrum, the half bandwidth of which is related to σ_{2s} as $\Delta\omega_{abs} = 2\sqrt{2\sigma_{2s}\ln 2}$. According to Refs. 13 and 14, the

following times are characteristic for the time evolution of the system under consideration: $\sigma_{2s}^{-1/2} < T' << \tau_s$, where $\sigma_{2s}^{-1/2}$ and $T' = (\tau_s/\sigma_{2s})^{1/3}$ are the times of reversible and irreversible dephasing of the electronic transition, respectively. The characteristic frequency range of changing the optical transition probability can be evaluated as the inverse T', i.e. $(T')^{-1}$. Thus, one can consider T' as a time of the optical electronic transition. Therefore, the inequality $\tau_s \gg T'$ implies that the optical transition is instantaneous where relation $T'/\tau_s << 1$ plays the role of a small parameter. This made it possible to describe vibrationally non-equilibrium populations in electronic states 1 and 2 $\rho_{jj}(\alpha, t)$ ($j = 1, 2$) by balance equations for the intense pulse excitation (pulse duration $t_p > T'$) and solve the problem.[6–8,15] For brevity, we consider here only one vibronic transition related to a HFOA vibration. Generalization to the case of a number of vibronic transitions will be made below.

The equation under discussion were written for the partial density matrix of the system $\rho_{jj}(\alpha, t)$ that described the system distribution in states 1 and 2 with a given value of α at time t. The complete density matrix averaged over the stochastic process which modulates the system energy levels, is obtained by integration of $\rho_{ij}(\alpha, t)$ over α, $\langle\rho\rangle_{ij}(t) = \int \rho_{ij}(\alpha, t)d\alpha$, where quantities $\langle\rho\rangle_{jj}(t)$ are the normalized populations of the corresponding electronic states: $\langle\rho\rangle_{jj}(t) \equiv n_j$, $n_1 + n_2 = 1$. Knowing $\rho_{jj}(\alpha, t)$, one can calculate the positive frequency component of the polarization $\mathbf{P}^{(+)}(t) = N\mathbf{D}_{12}\langle\rho\rangle_{21}(t)$, and the susceptibility $\chi(\Omega, t)$[6] that enables us to obtain the dielectric function ε due to relation $\varepsilon(\Omega, t) = 1 + 4\pi\chi(\Omega, t)$. Here N is the density of molecules, and $\mathbf{D}_{12}$ is the electronic matrix element of the dipole moment operator. It is worthy to note that magnitude $\varepsilon(\Omega, t)$ does make sense, since it changes in time slowly with respect to dephasing. In other words, $\varepsilon(\Omega, t)$ changes in time slowly with respect to reciprocal characteristic frequency domain of changing $\varepsilon(\Omega)$.

Let us include now the dipole-dipole intermolecular interactions in the condensed matter that are described by Hamiltonian[12,16,17]

$$H_{int} = \hbar \sum_{m \neq n} J_{mn} b_m^{\dagger} b_n \tag{3}$$

where J_{mn} is the resonant exciton coupling. Then Eq. (6) of Ref. 6 describing vibrationally non-equilibrium populations in electronic states $j = 1, 2$ for the exponential correlation function $K(t)/K(0) \equiv S(t) = \exp(-|t|/\tau_s)$ can be written as

$$\frac{\partial}{\partial t}\rho_{jj}(\alpha, t) = -i\hbar^{-1}[H_0(\alpha, t) + H_{int} - \mathbf{D} \cdot \mathbf{E}(t), \rho(\alpha, t)]_{jj} + L_{jj}\rho_{jj}(\alpha, t) \tag{4}$$

where $j = 1, 2$, and we added the term H_{int} into the Hamiltonian; the operator L_{jj} is determined by the equation:

$$L_{jj} = \tau_s^{-1}[1 + \left(\alpha - \delta_{j2}\omega_{st}\right)\frac{\partial}{\partial\left(\alpha - \delta_{j2}\omega_{st}\right)} + \\ + \sigma_{2s}\frac{\partial^2}{\partial\left(\alpha - \delta_{j2}\omega_{st}\right)^2}], \tag{5}$$

describes the diffusion with respect to the coordinate α in the corresponding effective parabolic potential $U_j(\alpha)$, δ_{ij} is the Kronecker delta, $\omega_{st} = \beta\hbar\sigma_{2s}$ is the Stokes shift of the equilibrium absorption and luminescence spectra, $\beta = 1/k_B T$. In the absence of the dipole-dipole intermolecular interactions in the condensed matter, H_{int}, Eq. (4) is reduced to Eq. (11) of Ref. 6.

Let us discuss the contribution of Hamiltonian $\hat{H}_{int}$ to the change of $\rho_{ij}(\alpha, t)$ in time. In other words, we shall generalize Eq. (11) of Ref. 6 to the dipole-dipole intermolecular interactions in the condensed matter. Using the Heisenberg equations of motion, one obtains that $\hat{H}_{int}$ gives the following contribution to the change of the expectation value of excitonic operator b_k in time

$$\frac{d}{dt}\langle b_k\rangle \sim \frac{i}{\hbar}\langle[\hat{H}_{int}, b_k]\rangle \equiv \frac{i}{\hbar}Tr([\hat{H}_{int}, b_k]\rho) \\ = -i\sum_{n \neq k} J_{kn}\langle(\hat{n}_{k1} - \hat{n}_{k2})b_n\rangle \tag{6}$$

where $\hat{n}_{k1} = b_k b_k^{\dagger}$, and $\hat{n}_{k2} = b_k^{\dagger} b_k$ is the exciton population operator. Considering an assembly of identical molecules, one can write $\langle b_k\rangle = \rho_{21}(\alpha, t)$[18] if averaging in Eq. (6) is carried out using

density matrix $\rho(\alpha,t)$. Consider the expectation value $\langle(\hat{n}_{k1}-\hat{n}_{k21})b_n\rangle = Tr[(\hat{n}_{k1}-\hat{n}_{k2})b_n\rho(\alpha_k,\alpha_n,t)]$ for $n\neq k$ where α_m is the effective vibrational coordinate of a molecule m ($m = k, n$). Due to fast dephasing (see above), it makes sense to neglect all correlations among different molecules,[12] and set $\langle(\hat{n}_{k1}-\hat{n}_{k2})b_n\rangle = \langle\hat{n}_{k1}-\hat{n}_{k2}\rangle\langle b_n\rangle$ and correspondingly $\rho(\alpha_k,\alpha_n,t)\simeq\rho(\alpha_k,t)\rho(\alpha_n,t)$, i.e. density matrix $\rho(\alpha_k,\alpha_n,t)$ is factorized. Here from dimension consideration one expectation value should be calculated using density matrix $\rho(\alpha,t)$, and another one - using $\langle\rho\rangle(t) = \int\rho(\alpha,t)d\alpha$. Since we sum with respect to n, it would appear reasonable to integrate with respect to α_n. However, this issue is not so simple. The point is that in addition to intramolecular vibrations, there is a contribution of low-frequency intermolecular and solvent coordinates into effective coordinate α. Because of this, partitioning the vibrations into α_k and α_n groups is ambiguous, and the mean-field approximation gives two options

$$p\langle b\rangle\langle\hat{n}_1-\hat{n}_2\rangle = \begin{pmatrix} p\rho_{21}(\alpha,t)\Delta n \\ p\langle\rho_{21}\rangle(t)\Delta'(\alpha,t)\end{pmatrix} \tag{7}$$

where $\Delta'(\alpha,t) = \rho_{11}(\alpha,t)-\rho_{22}(\alpha,t)$, $p\equiv-\sum_{n\neq k}J_{kn}$, $\Delta n\equiv n_1-n_2$. Below we shall discuss which option better corresponds to a specific experimental situation. Consideration based on non-equilibrium Green functions (GF) shows that the terms $p\rho_{21}(\alpha,t)$ and $p\langle\rho_{21}\rangle(t)$ on the right-hand-side of Eq. (7) represent the self-energy, $i\Sigma_{21}(t)$, and the terms Δn and $\Delta'(\alpha,t)$ - the difference of the "lesser" GFs for equal time arguments, $(i\hbar/N)[G^<_{11}(t,t)-G^<_{22}(t,t)]$, that are the density matrix, i.e. $p\langle b\rangle\langle\hat{n}_1-\hat{n}_2\rangle = -(\hbar/N)\Sigma_{21}(t)[G^<_{11}(t,t)-G^<_{22}(t,t)]$, respectively. In other words, for the first line on the right-hand-side of Eq. (7), the self-energy depends on α and the "lesser" GFs $G^<_{11}(t,t)-G^<_{22}(t,t)$ do not. In contrast, for the second line on the right-hand-side of Eq. (7), the self-energy does not depend on α and the "lesser" GFs $G^<_{11}(\alpha;t,t)-G^<_{22}(\alpha;t,t)$ do depend. This yields $\partial\rho_{21}(\alpha,t)/\partial t\sim-(i\hbar/N)\Sigma_{21}(t)[G^<_{11}(t,t)-G^<_{22}(t,t)]$. Adding term "$-(i\hbar/N)\Sigma_{21}(t)[G^<_{11}(t,t)-G^<_{22}(t,t)]$" to the right-hand side of Eq. (9) of Ref. 6 for the non-diagonal density matrix $\tilde{\rho}_{21}(\alpha,t)$

$$\frac{\partial}{\partial t}\tilde{\rho}_{21}(\alpha,t)+i(\omega_{21}-\omega-\alpha)\tilde{\rho}_{21}(\alpha,t)\approx\frac{i}{2\hbar}\mathbf{D}_{21}\cdot\mathbf{E}(t)\Delta'(\alpha,t)-\frac{i\hbar}{N}\tilde{\Sigma}_{21}(t)[G^<_{11}(t,t)-G^<_{22}(t,t)] \tag{8}$$

where ω_{21} is the frequency of Franck-Condon transition $1\rightarrow2$, $\tilde{\rho}_{21} = \rho_{21}\exp(i\omega t)$, $\tilde{\Sigma}_{21} = \Sigma_{21}\exp(i\omega t)$, and using the procedure described there, we get the extensions of Eq. (11) of Ref. 6 to the dipole-dipole intermolecular interactions in the condensed matter.

A. Self-energy depending on effective vibrational coordinate α

Consider first the case of self-energy depending on effective vibrational coordinate α (the first line on the right-hand-side of Eq. (7)) when the main contribution to α is due to low-frequency intermolecular vibrations and solvent coordinates. Then Eq. (8) becomes

$$\frac{\partial}{\partial t}\tilde{\rho}_{21}(\alpha,t)+i(\omega_{21}-\omega-p\Delta n-\alpha)\tilde{\rho}_{21}(\alpha,t)\approx\frac{i}{2\hbar}\mathbf{D}_{21}\cdot\mathbf{E}(t)\Delta'(\alpha,t) \tag{9}$$

Solving Eq. (9) for $\tilde{\rho}_{21}(\alpha,t)$ and substituting for the corresponding expression in Eq. (4), we arrive to equation

$$\frac{\partial\rho_{jj}(\alpha,t)}{\partial t} = L_{jj}\rho_{jj}(\alpha,t)+\frac{(-1)^j\pi}{2}\Delta'(\alpha,t)|\Omega_R(t)|^2\times \\ \times\delta[\omega_{21}-p\Delta n-\omega-\alpha] \tag{10}$$

that was obtained in Ref. 19. Here ω_{21} is the frequency of Franck-Condon transition $1\rightarrow2$, $\Omega_R(t) = (\mathbf{D}_{12}\cdot\mathbf{e})\mathcal{E}(t)/\hbar$ is the Rabi frequency, $\mathbf{D}_{12}$ is the electronic matrix element of the dipole moment operator. In that case, as one can see from Eq. (10), the self-energy $i\Sigma_{21}(t) = p\rho_{21}(\alpha,t)$ results in the frequency shift of spectra " $-p\Delta n$" without changing the line shapes. One can show that this approach correctly describes the change of the first moment of optical spectra in the condensed matter. Calculations of p for isotropic medium give $p = \frac{4\pi}{3\hbar}|D_{12}|^2N > 0$[12,19] that corresponds to a red shift, according to the Clausius-Mossotti Lorentz-Lorentz (CMLL) mechanism.[9]

Integration of Eq. (10) is achieved by the Green's function[15]

$$G_{jj}(\alpha,t;\alpha',t')=\frac{1}{\sqrt{2\pi\sigma(t-t')}}\exp\{-[(\alpha-\delta_{j2}\omega_{st})-(\alpha'-\delta_{j2}\omega_{st})S(t-t')]^2/(2\sigma(t-t'))\} \quad (11)$$

where $\sigma(t-t')=\sigma_{2s}[1-S^2(t-t')]$, for the initial condition,

$$\rho_{jj}^{(0)}(\alpha)\equiv\rho_{jj}(\alpha,t=0)=\delta_{j1}(2\pi\sigma_{2s})^{-1/2}\exp(-\frac{\alpha^2}{2\sigma_{2s}}) \quad (12)$$

We obtain

$$\begin{aligned}\rho_{jj}(\alpha,t)=\rho_{jj}^{(0)}(\alpha)+(-1)^j\frac{\pi}{2}\\ \times\int_0^t dt'|\Omega_R(t')|^2\Delta'(\omega_{21}-p\Delta n-\omega,t')\\ \times G_{jj}(\alpha,t;\omega_{21}-p\Delta n-\omega,t')\end{aligned} \quad (13)$$

where $\Delta'(\omega_{21}-p\Delta n-\omega,t')$ satisfies nonlinear integral equations that can be easily obtained from Eq. (13). Integrating both sides of Eq. (13) with respect to α and bearing in mind that $\int_{-\infty}^{\infty}G_{jj}(\alpha,t;\omega_{21}-\omega(t'),t')d\alpha=1$, we get

$$\frac{dn_j}{dt}=(-1)^j\frac{\pi}{2}|\Omega_R(t)|^2\Delta'(\omega_{21}-p\Delta n-\omega,t) \quad (14)$$

1. Fast vibrational relaxation

Let us consider the particular case of fast vibrational relaxation when one can put the normalized correlation function $S(t-t')\equiv K(t-t')/K(0)$ equal to zero. Physically it means that the equilibrium distributions into the electronic states have had time to be set during changing the pulse parameters. Bearing in mind that for fast vibronic relaxation

$$\begin{aligned}\Delta'(\alpha,t)=\frac{n_1(t)}{(2\pi\sigma_{2s})^{1/2}}\exp(-\frac{\alpha^2}{2\sigma_{2s}})-\\ -\frac{n_2(t)}{(2\pi\sigma_{2s})^{1/2}}\exp[-\frac{(\alpha-\omega_{st})^2}{2\sigma_{2s}}],\end{aligned} \quad (15)$$

substituting the last equation into Eq. (14), one gets the equations for the populations of electronic states $n_{1,2}$

$$\begin{aligned}\frac{dn_j}{dt}=(-1)^j\sigma_a(\omega_{21})\tilde{J}(t)\mathrm{Re}\,[n_1\bar{W}_a(\omega+p\Delta n)-\\ -n_2\bar{W}_f(\omega+p\Delta n)]-(-1)^j\frac{n_2}{T_1}\end{aligned} \quad (16)$$

where $n_1+n_2=1$, σ_a is the cross section at the maximum of the absorption band, $\tilde{J}(t)$ is the power density of exciting radiation, $\bar{W}_{a(f)}(\omega)=W_{a(f)}(\omega)/F_{a,\max}$, $F_{a,\max}$ is the maximum value of the absorption line (see below), and we added term "$(-1)^j n_2/T_1$" taking the lifetime T_1 of the excited state into account. Here " $-iW_{a(f)}(\omega)$" is the line-shape function of a monomer molecule for the absorption (fluorescence) for fast vibronic relaxation. In the case under consideration, it is related to the line-shape function, $\int d\alpha\Delta'(\alpha,t)\zeta(\omega-\omega_{21}+\alpha)/\pi$, by formula

$$\int_{-\infty}^{\infty}d\alpha\Delta'(\alpha,t)\zeta(\omega-\omega_{21}+\alpha)/\pi=-i[n_1(t)W_a(\omega)-n_2(t)W_f(\omega)] \quad (17)$$

where $\zeta(\omega-\omega_{21}+\alpha)=\frac{P}{\omega-\omega_{21}+\alpha}-i\pi\delta(\omega-\omega_{21}+\alpha)$, P is the symbol of the principal value.

The imaginary part of " $-iW_{a(f)}(\omega)$" with sign minus, $-\mathrm{Im}[-iW_{a(f)}(\omega)]=\mathrm{Re}W_{a(f)}(\omega)\equiv F_{a(f)}(\omega)$, describes the absorption (fluorescence) lineshapes of a monomer molecule, and the real part, $\mathrm{Re}[-iW_{a(f)}(\omega)]=\mathrm{Im}W_{a(f)}(\omega)$, describes the corresponding refraction spectra. For the "slow modulation" limit considered in the beginning of this section, quantities $W_{a(f)}(\omega)$ and $F_{a(f)}(\omega)$ are given by

$$W_{a(f)}(\omega)=\sqrt{\frac{1}{2\pi\sigma_{2s}}}w(\frac{\omega-\omega_{21}+\delta_{a(f),f}\omega_{st}}{\sqrt{2\sigma_{2s}}}) \quad (18)$$

where $w(z) = \exp(-z^2)[1 + i\mathrm{erfi}(z)]$ is the probability integral of a complex argument,[20] and

$$F_{a(f)}(\omega) = \sqrt{\frac{1}{2\pi\sigma_{2s}}}\exp[-\frac{\left(\omega_{21} - \omega - \delta_{a(f),f}\omega_{st}\right)^2}{2\sigma_{2s}}] \tag{19}$$

Eq. (16) was applied to the optical control of Coulomb blocking in nanojunctions and switching waves in bistable organic thin films, in Refs. 19 and 21, respectively.

B. Population difference ("lesser" GFs) depending on effective vibrational coordinate α

Consider now the case when the population difference depends on effective vibrational coordinate α (the second line on the right-hand-side of Eq. (7); the main contribution to α is due to intramolecular vibrations). Then using Eqs. (4) and (8), we arrive to equation

$$\frac{\partial\rho_{jj}(\alpha,t)}{\partial t} = L_{jj}\rho_{jj}(\alpha,t) + \frac{(-1)^j\pi}{2}\Delta'(\alpha,t) \times \delta(\omega_{21} - \omega - \alpha)|\Omega_{eff}(t)|^2 \tag{20}$$

where $\Omega_{eff}(t) = \Omega_R(t) + 2p\langle\rho_{21}\rangle(t) = \Omega_R(t) + 2i\Sigma_{21}(t)$ is the effective Rabi frequency that can be written as

$$\Omega_{eff}(t) = \frac{\Omega_R(t)}{1 + p\int d\alpha\Delta'(\alpha,t)\zeta(\omega - \omega_{21} + \alpha)}, \tag{21}$$

One can see that in contrast to the self-energy depending on effective vibrational coordinate α (see above), here the self-energy $\Sigma_{21}(t) = -ip\langle\rho_{21}\rangle(t)$ (the second line on the right-hand-side of Eq. (7)) results in the change of both the frequency shift of spectra and their lineshapes. In that case considering the dense collection of molecules under the action of one more (weak) field

$$\tilde{\mathbf{E}}(t) = \frac{1}{2}\mathbf{e}\tilde{\mathcal{E}}(t)\exp(-i\Omega t) + \text{c.c.},$$

one gets for the positive frequency component of the polarization $\mathbf{P}^+ = N\mathbf{D}_{12}\langle\rho_{21}\rangle(t)$

$$\mathbf{P}^+(\Omega,t) = \frac{-N\mathbf{D}_{12}(\mathbf{D}_{21}\cdot\mathbf{e})\eta\tilde{\mathcal{E}}(t)/(2\hbar)}{[\int d\alpha\Delta'(\alpha,t)\zeta(\Omega - \omega_{21} + \alpha)]^{-1} + p}, \tag{22}$$

for the susceptibility

$$\chi(\Omega,t) = -\frac{N\eta|D_{12}|^2}{\hbar}\frac{\int d\alpha\Delta'(\alpha,t)\zeta(\Omega - \omega_{21} + \alpha)}{1 + p\int d\alpha\Delta'(\alpha,t)\zeta(\Omega - \omega_{21} + \alpha)} \tag{23}$$

and the dielectric function $\varepsilon(\Omega) = \varepsilon_0(1 + 4\pi\chi(\Omega))$[22] that in our case is given by

$$\varepsilon(\Omega,t) = \varepsilon_0[1 - \frac{q\int d\alpha\Delta'(\alpha,t)\zeta(\Omega - \omega_{21} + \alpha)}{1 + p\int d\alpha\Delta'(\alpha,t)\zeta(\Omega - \omega_{21} + \alpha)}] \tag{24}$$

where $\varepsilon_0 = n_0^2$, n_0 is the background refractive index of the medium, $q \equiv 4\pi\eta\frac{N|\mathbf{D}_{12}|^2}{\hbar}$, $\eta = 1/3$ for randomly oriented molecules, and $\eta = 1$ for the molecules of the same orientation.

1. Line-shape in the fast vibrational relaxation limit

Below we shall see that the approximation based on the self-energy integrated on the effective vibrational coordinate (the second line on the right-hand-side of Eq. (7)) correctly describe the exciton spectra. In that case the fast vibrational relaxation limit should be based on the equilibrium state of the collective system (molecules coupled by the dipole-dipole interaction). However, the

exciton wave function in the ground state is the product of the wave functions of monomers[16] (no intermolecular interactions). Because of this, for the absorption of weak radiation, one should put $j = 1$ and $\Delta'(\alpha, t) = \Delta'^{(0)}(\alpha)$ in Eqs. (20) and (21) where $\Delta'^{(0)}(\alpha) = \rho_{11}^{(0)}(\alpha) = (2\pi\sigma_{2s})^{-1/2} \exp[-\alpha^2/(2\sigma_{2s})]$ is the equilibrium value of $\Delta'(\alpha, t)$ corresponding to the equilibrium value for a monomer in the ground state, and we retained only terms that are proportional to $|\Omega_R(t)|^2$ on the right-hand side of Eq. (20). The next procedure is similar to that used for obtaining Eq. (16). Integrating Eq. (20), using Green function, Eq. (11), we obtain an integral equation that is similar to Eq. (13). Then integrating both sides of the obtained integral equation with respect to α, and bearing in mind Eq. (17), we get

$$\frac{dn_1}{dt} = -\sigma_a(\omega_{21})\tilde{J}(t)\mathrm{Re}\frac{\bar{W}_a(\omega)}{1 - ip\pi W_a(\omega)} + \frac{n_2}{T_1} \tag{25}$$

where the term $\mathrm{Re}\{\bar{W}_a(\omega)/[1-ip\pi W_a(\omega)]\}$ describes the absorption spectrum of molecules susceptible to the dipole-dipole intermolecular interactions expressed through their monomer spectra W_a.

a. Description of the absorption of J-aggregates. Applying expression $\mathrm{Re}\{\bar{W}_a(\omega)/[1-ip\pi W_a(\omega)]\}$ on the right-hand-side of Eq. (25) to the description of the absorption of J-aggregates, one should take into account that the Gaussian shape of the monomer absorption spectrum obtained in the "slow modulation" limit, Eq. (19), is correct only near the absorption maximum. The wings decline much slower as $(\omega_{21} - \omega)^{-4}$.[23] At the same time, the expression under discussion has a pole, giving strong absorption, when $1/(p\pi) = -\mathrm{Im}W_a(\omega)$. If parameter of the dipole-dipole intermolecular interaction p is rather large, the pole may be at a large distance from the absorption band maximum where the "slow modulation" limit breaks down. This means one should use exact expression for the monomer spectrum W_a that is not limited by the "slow modulation" approximation, and properly describes both the central spectrum region and its wings. The exact calculation of the vibrationally equilibrium monomer spectrum for the Gaussian-Markovian modulation with the exponential correlation function $S(t) = \exp(-|t|/\tau_s)$ gives[23,24] (see Eqs. (A3) and (A4) of the Appendix)

$$W_a(\omega) = \frac{\tau_s}{\pi}\frac{\Phi(1, 1 + x_a; \sigma_{2s}\tau_s^2)}{x_a} \tag{26}$$

where $x_a = \tau_s/(2T_1) + \sigma_{2s}\tau_s^2 + i\tau_s(\omega_{21} - \omega)$, $\Phi(1, 1+x_a; \sigma_{2s}\tau_s^2)$ is a confluent hypergeometric function.[20]

Figs. 1 and 2 show the calculation results of the absorption spectra of J-aggregates according to the expression $\mathrm{Re}\{W_a(\omega)/[1 - ip\pi W_a(\omega)]\}$ on the right-hand side of Eq. (25) and Eq. (26), and their comparison with the monomer spectra $\mathrm{Re}W_a(\omega)$. The spectra of Fig. 1 correspond to the slow modulation case with parameters close to those of molecule LD690:[6] $\sqrt{\sigma_{2s}} = 546\ cm^{-1}$, $\tau_s = 10^{-13}s$ that gives $\omega_{st} = 1420\ cm^{-1}$. We put $T_1 = 10^{-9}s$.

One can see that in spite of strong narrowing the J-aggregate spectra with respect to those of monomers, the vibrations still give rather important contribution to broadening the J-aggregate spectra that may be crucial. Indeed, the half bandwidth of the J-aggregate absorption spectrum is about $3 \cdot 10^{12}\ rad/s$ that may far exceed the lifetime contribution. So, disregarding vibrations in the description of the J-aggregate spectra may be incorrect. Moreover, above parameters for molecule

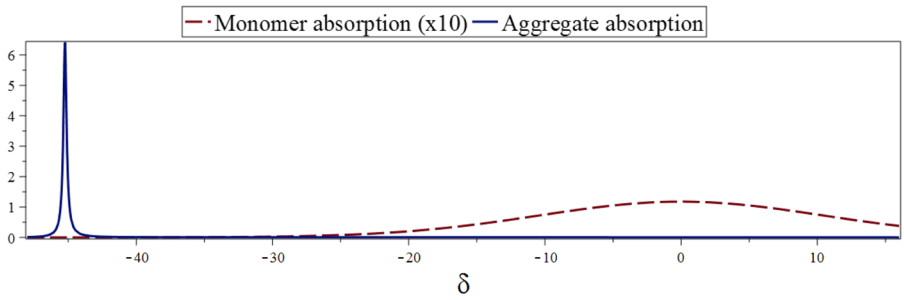

FIG. 1. Absorption spectra (in terms of τ_s/π) of the J-aggregate (solid line) and the corresponding monomer (dashed line) in the case of slow modulation ($\sqrt{\sigma_{2s}}\tau_s = 10.9 >> 1$) and $p\tau_s = 42$. Dimensionless parameter is $\delta = \tau_s(\omega - \omega_{21})$.

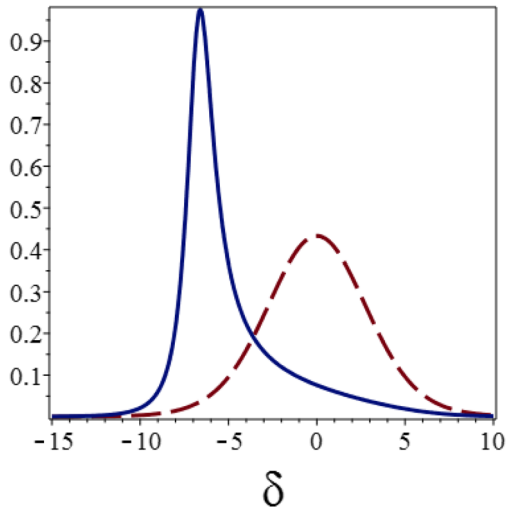

FIG. 2. Absorption spectra (in terms of τ_s/π) of the J-aggregate (solid line) and the corresponding monomer (dashed line) for $\sqrt{\sigma_{2s}}\tau_s = 3.16$ and $p\tau_s = 5$.

LD690 in methanol were obtained using only LFOA vibrations $\{\omega_s\}$ for the simulation of its spectra.[6] If one in addition uses also high frequency OA intramolecular vibrations (like C-C ~ 1400 cm^{-1}) for the simulation (see below), then the second central moment σ_{2s} should be related rather to a vibronic transition with respect to the high frequency OA vibration than to the whole spectrum, i.e. the value of σ_{2s} diminishes. Fig. 2 shows absorption spectra of the J-aggregate and the corresponding monomer when parameter $\sqrt{\sigma_{2s}}\tau_s = 3.16$ is smaller than that for Fig. 1. One can see lesser narrowing the J-aggregate spectrum with respect to that of a monomer. In contrast, the J-aggregate absorption spectrum calculated using the monomer spectrum W_a, Eq. (18), and, as a consequence, the Gaussian absorption spectrum, Eq. (19), is extremely narrow.

For fast modulation when $\sigma_{2s}\tau_s^2 << 1$, the aggregate spectrum only shifts with respect to the monomer one without changing its shape. Indeed, $\Phi(1, 1 + x_{a(f)}; \sigma_{2s}\tau_s^2) \approx 1$ for $\sigma_{2s}\tau_s^2 << 1$. In that case $W_a(\omega) \approx (\tau_s/\pi)/x_a$, and the term $\mathrm{Re}\{\bar{W}_a(\omega)/[1 - ip\pi W_a(\omega)]\}$ on the right-hand side of Eq. (25) becomes

$$\mathrm{Re}\frac{W_a(\omega)}{1 - ip\pi W_a(\omega)} \approx \frac{1}{\pi}\mathrm{Re}\frac{1}{\frac{1}{2T_1} + \sigma_{2s}\tau_s + i(\omega_{21} - \omega - p)} = W_a(\omega + p) \tag{27}$$

In other words, if the monomer spectrum has Lorentzian shape, the aggregate spectrum is simply shifted monomer spectrum. In that case both the approach based on the self-energy depending on the effective vibrational coordinate, and the approach based on the population difference ("lesser" GFs) depending on the effective vibrational coordinate give the same absorption spectrum of molecules susceptible to the dipole-dipole intermolecular interactions.

b. J-aggregates under stronger radiation. Touching on how Eq. (25) can be extended to stronger radiation, one should recognize two limit cases. In the first case an optical transitions occur near zero quasi-momentum $\mathbf{k} \approx 0$. After the light absorption a quasi-equilibrium is established. However, the luminescence should be resonant to the absorption line due to the quasi-momentum conservation.[16] This case is realized for J-aggregates.[25] The second case is characterized by a strong electron-vibrational interaction when the relaxation to the equilibrium vibrational configuration in the excited state occurs before the excitation transfers to the neighboring molecule.[26] It seems such a case is realized for the H-aggregates of thiacyanine (TC) dye molecules where a large Stokes shift between absorption and photoluminescence spectra of the TC aggregates was observed in the aqueous solution.[27,28] Since the description of the H-aggregate spectra necessitates including also the HFOA vibrations and the mechanism described by Eq. (16) (see Section III), the extension to stronger radiation for H-aggregates will be carried out elsewhere.

For the first case one can put $\Delta'(\alpha,t)=\Delta n(2\pi\sigma_{2s})^{-1/2}\exp[-\alpha^2/(2\sigma_{2s})]$ in Eqs. (20) and (21), and we obtain the extension of Eq. (25) to stronger radiation

$$\frac{dn_1}{dt}=-\sigma_a(\omega_{21})\tilde{J}(t)\mathrm{Re}\frac{\Delta n\bar{W}_a(\omega)}{1-ip\pi\Delta nW_a(\omega)}+\frac{n_2}{T_1} \tag{28}$$

In Eq. (28) the probability of the light induced transitions may be of the same order of magnitude as T_1^{-1}, however, the first should be smaller than the reciprocal dephasing time.

The term "$\mathrm{Re}\frac{\Delta n\bar{W}_a(\omega)}{1-ip\pi\Delta nW_a(\omega)}$" on the right-hand-side of Eq. (28) describes a nonlinear absorption. In particular case of weak radiation when $\Delta n=1$, this term recovers the coherent exciton scattering (CES) approximation.[10,29,30] The latter is well suited to describing the absorption spectrum lineshape for J-aggregates using their monomer spectra and the intermolecular interaction strength that is a fitting parameter. As to the absorption spectra of H-aggregates, the CES approximation describes correctly only their lineshapes. The positions of the H-aggregate spectra calculated in the CES approximation should be corrected.[10] This issue will be considered in more details in Section III, since we apply our theory to the EPs in H-aggregates of TC dye molecules below.

It is worthy to note that the term $1/[1-ip\pi W_a(\omega)]$ on the right-hand side of Eq. (25) (and the corresponding term on the right-hand side of Eq. (28) for $\Delta n=1$) amounts to the Pade approximant [0/1][31] that is the sum of diagrams of a certain type.[32] Indeed, the term under discussion is the sum of the infinite geometrical series

$$\frac{1}{1-ip\pi W_a(\omega)}=\sum_{m=0}^{\infty}p^m[i\pi W_a(\omega)]^m \tag{29}$$

where the right-hand side of Eq. (29) multiplied by $W_a(\omega)$ may be considered as a Born series with the interaction parameter p.

Fig. 3 shows the calculation results of the nonlinear absorption spectra of J-aggregates according to the expression $\mathrm{Re}\{\Delta nW_a(\omega)/[1-ip\pi\Delta nW_a(\omega)]\}$ on the right-hand-side of Eq. (28) for different values of the population difference Δn. The vibrationally equilibrium monomer absorption spectrum $W_a(\omega)$ was calculated using Eq. (26). The spectra of Fig. 3 demonstrate the saturation effect accompanied by the blue shift of the spectra when the population difference Δn diminishes. Such a frequency shift arises also in the many-body theory of 1D Frenkel excitons[33] that does not consider the vibrations. In contrast, our theory does take the vibrations into account that enables us to correctly describe the lineshape of J-aggregates.

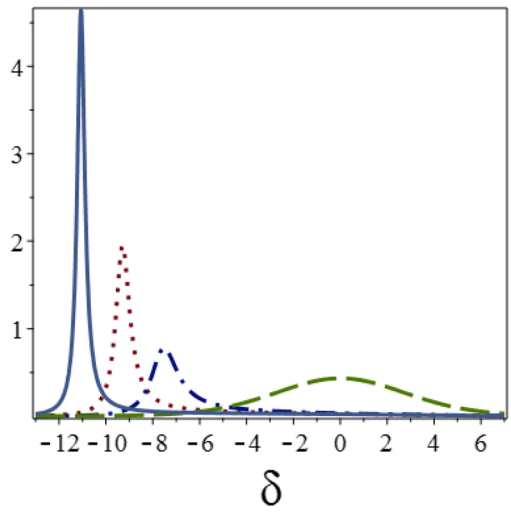

FIG. 3. Nonlinear absorption spectra (in terms of τ_s/π) of the J-aggregate for $\Delta n=1$ (solid line), $\Delta n=0.8$ (dotted line), $\Delta n=0.6$ (dash dotted line), and the corresponding monomer absorption spectrum (dashed line) for $\sqrt{\sigma_{2s}}\tau_s=3.16$ and $p\tau_s=10$. Dimensionless parameter is $\delta=\tau_s(\omega-\omega_{21})$, $\tau_s/(2T_1)<<1$.

III. PROPER DESCRIPTION OF THE LINESHAPE AND THE FREQUENCY SHIFT OF ABSORPTION SPECTRA OF H-AGGREGATES

Applying expression $\mathrm{Re}\{W_a(\omega)/[1 - ip\pi W_a(\omega)]\}$ (see Section II B 1) to the description of the absorption of H-aggregates, one should take into account also HFOA intramolecular vibrations, in addition to the LFOA vibrations $\{\omega_s\}$ under consideration in our paper. The intramolecular relaxation related to the OAHF vibrations takes place in a time shorter than intermolecular relaxation of the low frequency system $\{\omega_s\}$.[7,8,34–36] Therefore, we can consider the density matrix averaged with respect to the intramolecular OAHF vibrations:

$$\rho_{ns}(t) = Tr_M \rho_{nn}(t) \tag{30}$$

where the total density matrix $\rho_{nn}(t)$ is factorized

$$\rho_{nn}(t) = \rho_{nM} \rho_{ns}(t) \tag{31}$$

and

$$\rho_{nM} = \exp(-\beta W_{nM})/Tr_M \exp(-\beta W_{nM})$$

is the equilibrium density matrix of the intramolecular OAHF vibrations. Here Tr_M denotes the operation of taking a trace over the variables of the intramolecular OAHF vibrations, $\beta = 1/(k_B T)$. Using density matrix ρ_{ns}, one can obtain an equation akin to Eq. (25) that also contains expression $\mathrm{Re}\{W_a(\omega)/[1 - ip\pi W_a(\omega)]\}$ (see Section II B 1) for the description of the absorption of H-aggregates where the monomer spectrum W_a should include the contribution from the HFOA intramolecular vibrations. We will consider one normal high frequency intramolecular oscillator of frequency ω_0 whose equilibrium position is shifted under electronic transition. Its characteristic function $f_{\alpha M}(t)$ is determined by the following expression:[7,37]

$$f_{\alpha M}(t) = \exp(-S_0 \coth\theta_0) \sum_{k=-\infty}^{\infty} I_k(S_0/\sinh\theta_0) \times \exp[k(\theta_0 + i\omega_0 t)] \tag{32}$$

where S_0 is the dimensionless parameter of the shift, $\theta_0 = \hbar\omega_0/(2k_B T)$, $I_n(x)$ is the modified Bessel function of first kind.[20] Then the monomer spectrum can be written as $W_a(\omega) = (1/\pi)\int_0^\infty f^*_{\alpha M}(t) \exp[i(\omega - \omega_{21})t + g_s(t)]dt$ where $g_s(t)$ is given by Eq. (A4) of the Appendix. Integrating with respect to t, one gets

$$W_a(\omega) = \frac{\tau_s}{\pi} \exp(-S_0 \coth\theta_0) \sum_{k=-\infty}^{\infty} I_k\left(\frac{S_0}{\sinh\theta_0}\right) \times \exp(k\theta_0) \frac{\Phi(1, 1 + x_{ak}; \sigma_{2s}\tau_s^2)}{x_{ak}} \tag{33}$$

where $x_{ak} = \tau_s/(2T_1) + \sigma_{2s}\tau_s^2 + i\tau_s(\omega_{21} - \omega + k\omega_0)$. Eq. (33) is the extension of Eq. (26) to the presence of the HFOA intramolecular vibrations. For $\theta_0 >> 1$ we obtain

$$W_a(\omega) = \frac{\tau_s}{\pi} \exp(-S_0) \sum_{k=0}^{\infty} \frac{S_0^k}{k!} \frac{\Phi(1, 1 + x_{ak}; \sigma_{2s}\tau_s^2)}{x_{ak}} \tag{34}$$

As we mentioned above, expression $\mathrm{Re}\{W_a(\omega)/[1 - ip\pi W_a(\omega)]\}$ corresponds to the CES approximation that describes well the shape of the absorption spectra of H-aggregates. However, the spectra calculated in the CES approximation are blue shifted with respect to the experimental spectra of pinacyanol in aqueous solution at $20^\circ C$ and in aqueous solution with 7.5% v/v ethanol at room temperature.[10] To resolve the problem, the authors of Ref. 10 empirically introduced additional red shift that can be substantiated in our more general theory. Indeed, let us write down Eq. (8) when both the self-energy ($\sim \tilde{\rho}_{21}$) and the population difference depend on the effective vibrational coordinate

$$\frac{\partial}{\partial t}\tilde{\rho}_{21}(\alpha,t)+i(\omega_{21}-\omega-p_1-\alpha)\tilde{\rho}_{21}(\alpha,t)=i[\frac{\mathbf{D}_{21}\cdot\mathbf{E}(t)}{2\hbar}+p_2\int d\alpha\tilde{\rho}_{21}(\alpha,t)]\rho_{11}^{(0)}(\alpha) \tag{35}$$

Using the procedure described in Ref. 6, we get an equation similar to Eq. (20) (together with Eq. (21)) with the only difference that ω_{21} should be replaced by $\omega_{21}-p_1$, and p - by p_2

$$\frac{\partial\rho_{11}(\alpha,t)}{\partial t}=\frac{-\frac{\pi}{2}\rho_{11}^{(0)}(\alpha)|\Omega_R(t)|^2\delta(\omega_{21}-\omega-p_1-\alpha)}{\left|1+p_2\int d\alpha\rho_{11}^{(0)}(\alpha)\zeta(\omega+p_1-\omega_{21}+\alpha)\right|^2}+L_{11}\rho_{11}(\alpha,t) \tag{36}$$

Then similar to Eq. (25), we obtain

$$\frac{dn_1}{dt}=-\sigma_a(\omega_{21})\tilde{J}(t)\mathrm{Re}\frac{\bar{W}_a(\omega+p_1)}{1-ip_2\pi W_a(\omega+p_1)}+\frac{n_2}{T_1} \tag{37}$$

where the term $\mathrm{Re}\{\bar{W}_a(\omega+p_1)/[1-ip_2\pi W_a(\omega+p_1)]\}$ describes the absorption spectrum of molecules susceptible to the dipole-dipole intermolecular interactions expressed through their monomer spectra $W_a(\omega+p_1)$, Eq. (34) (see also Eq. (33)). Fig. 4 shows the calculation results of the absorption spectrum of an H-aggregate according to the expression $\mathrm{Re}\{W_a(\omega+p_1)/[1-ip_2\pi W_a(\omega+p_1)]\}$ on the right-hand side of Eq. (37) and Eq. (34) (solid line), and its comparison with the monomer spectrum $\mathrm{Re}W_a(\omega)$ (dash line) and the spectrum of H-aggregate, $\mathrm{Re}\{W_a(\omega)/[1-ip_2\pi W_a(\omega)]\}$, calculated without the contribution of the CMLL mechanism (dash dot line). The values of parameters are found by fitting the experimental spectrum of the linear absorption of LD690 in methanol:[8] $\tau_s=10^{-13}s$, $k_BT=210\ cm^{-1}$, $\hbar\omega_{st}/(2k_BT)=1.99$, $S_0=0.454$, $\omega_0=1130\ cm^{-1}$, $\sigma_{2s}=\omega_{st}k_BT/\hbar$. The spectra presented in Fig. 4 manifest that though the shape of the H-aggregate spectrum is fully described by the self-energy not depending on the effective vibrational coordinate, its position (including the additional red shift of the experimental spectra of H-aggregates[10]) may be correctly described only taking the CMLL mechanism into account. In other words, our more general theory enables us to describe both the shape and the position of the experimental spectra of H-aggregates due to the self-energy and the population difference ("lesser" GFs) both depending on the effective vibrational coordinate that leads to their frequency dependence. This can be understood as follows. The frequency dependent "lesser" GFs corresponding to the CES approximation describe well the spectral shapes of H-aggregates. The latters can interact with each other by the dipole-dipole interaction leading to the CMLL red shift that is described by the frequency dependent self-energy.

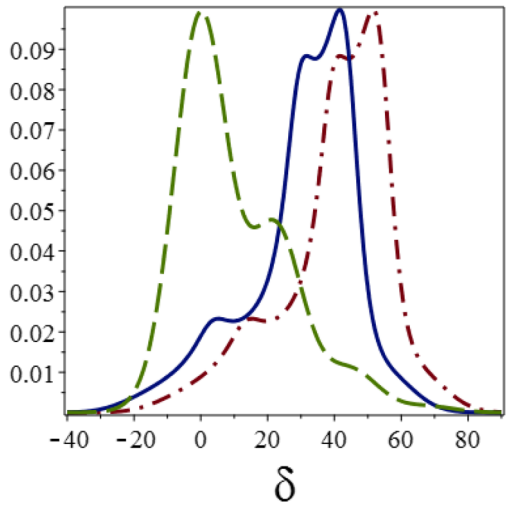

FIG. 4. Absorption spectra (in terms of τ_s/π) of the H-aggregate (solid line), the corresponding monomer (dash line) and the H-aggregate without the contribution of the CMLL mechanism (dash dot line) for $p_1=500\ cm^{-1}$ and $p_2=-1500\ cm^{-1}$ Dimensionless parameter is $\delta=\tau_s(\omega-\omega_{21})$.

In the case under consideration Eq. (24) for the dielectric function becomes

$$\varepsilon(\omega) = \varepsilon_0[1 + \frac{iq\pi W_a(\omega + p_1)}{1 - i\pi p_2 W_a(\omega + p_1)}] \tag{38}$$

where we put $\int_{-\infty}^{\infty} d\alpha \Delta'^{(0)}(\alpha)\zeta(\omega - \omega_{21} + p_1 + \alpha) = -i\pi W_a(\omega + p_1)$ for the vibrational equilibrium in the ground state.

IV. APPLICATION TO THE EXCITON-POLARITON EXPERIMENT

The theory developed in Section III properly describes both the lineshape and the frequency shift of the absorption spectra of H-aggregates. Therefore, it can be applied to the experiment on fraction of a millimeter propagation of EPs in photoexcited fiber-shaped H-aggregates of TC dye at room temperature.[4]

The transverse eigenmodes of the medium are obtained from the dispersion equation[22]

$$c^2k^2(\omega) = \omega^2\varepsilon(\omega) \tag{39}$$

where dielectric function $\varepsilon(\omega)$ is given by Eq. (38) and depends on the monomer spectra W_a.

Fig. 5 shows the experimental absorption lineshape of TC monomer solution prepared by dissolving TC dye in methanol[27] (top), and its theoretical description by ReW_a, Eq. (34), (bottom).

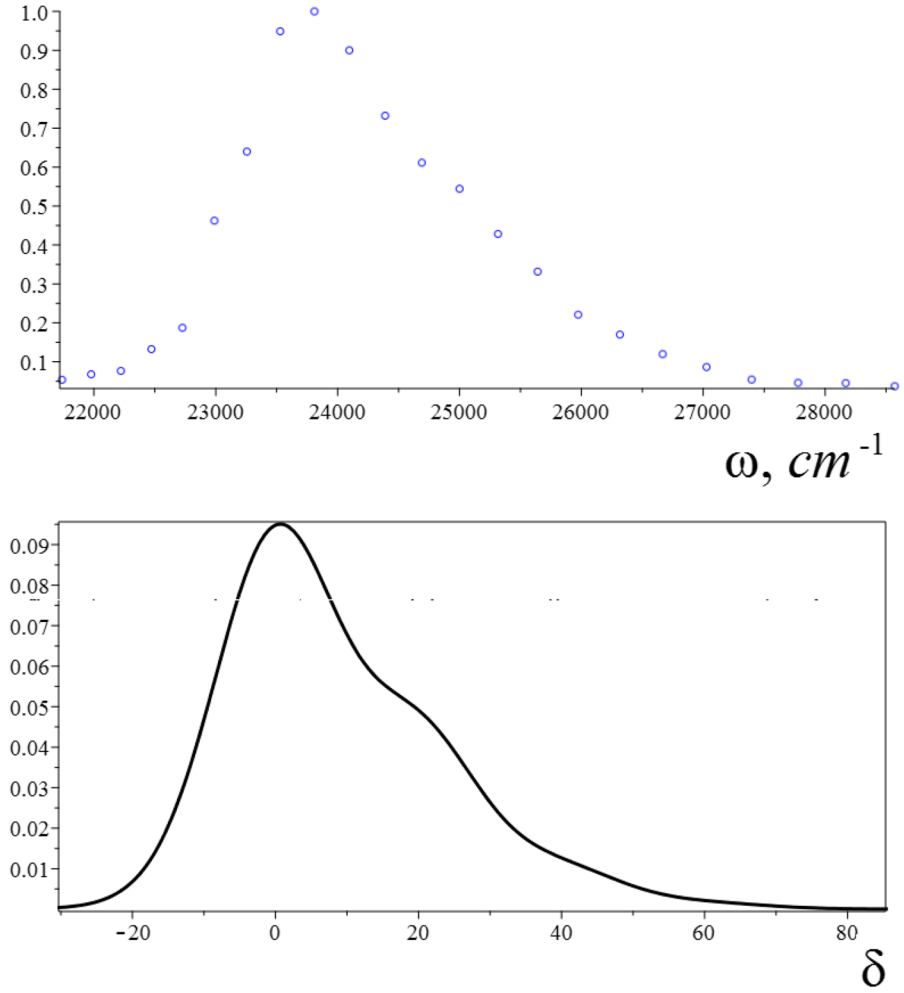

FIG. 5. Experimental absorption lineshape of TC monomer solution prepared by dissolving TC dye in methanol[27] (top), and its theoretical description (in terms of τ_s/π) by ReW_a, Eq. (34), (bottom).

Good agreement is observed with the values of parameters $\omega_{21} = 23810\ cm^{-1}$, $1/\tau_s = 75\ cm^{-1}$, $\omega_0\tau_s = 20$, $S_0 = 0.454$, $\sigma_{2s}\tau_s^2 = 80$ obtained by comparison between experimental and theoretical curves.

The monomer spectrum found, W_a, enables us to calculate the aggregate absorption spectrum according to the formula $\mathrm{Re}\{W_a(\omega + p_1)/[1 - ip_2\pi W_a(\omega + p_1)]\}$ (see Eqs. (37) and (38)) shown in Fig. 6. Again good agreement between theoretical and experimental spectra is observed with the values of parameters $p_1\tau_s = 4$, $p_2\tau_s = -7$ obtained by comparison between experimental and theoretical curves. We did not make additional fitting since experimental absorption spectra of TC aggregates and monomers were measured in different solvents[27] (see caption to Fig. 6).

A. Polariton dispersion

Let us analyze Eq. (39) where the dielectric function is determined by Eq. (38) and depends on the aggregate spectrum, $W_a(\omega + p_1)/[1 - ip_2\pi W_a(\omega + p_1)]$. The parameters of the aggregate spectrum

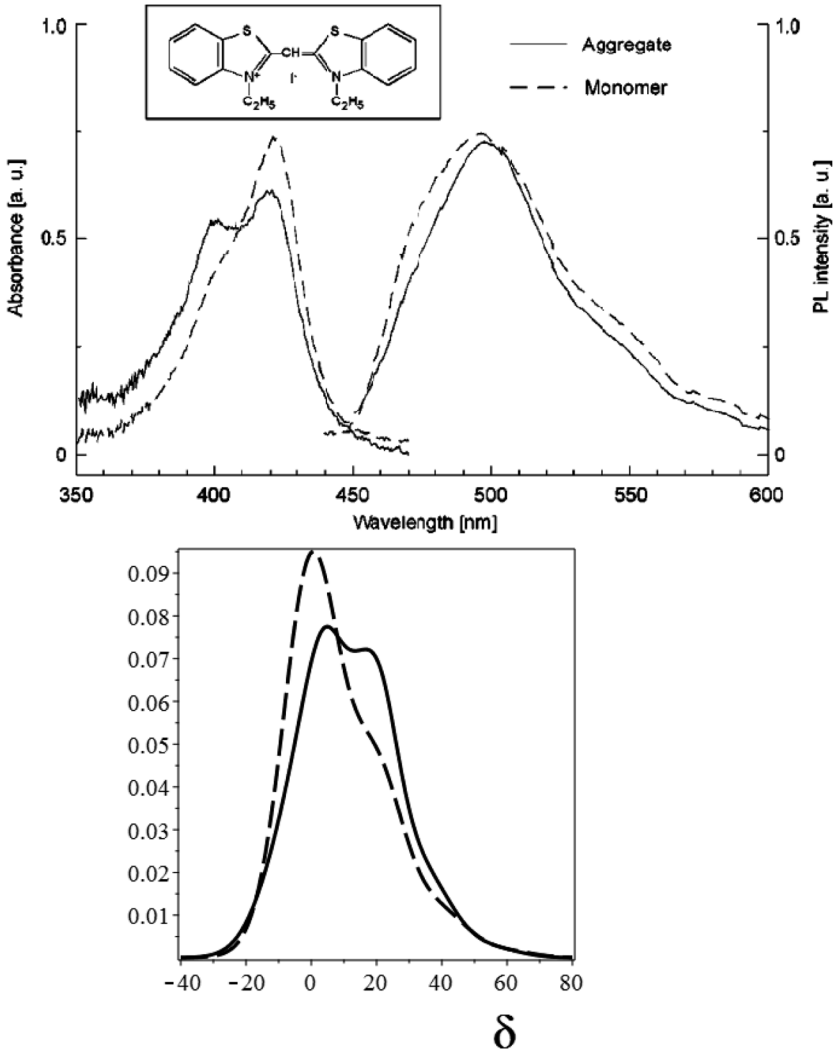

FIG. 6. Experimental absorption and photoluminescence spectra of TC aggregates and monomers[27] (top), and theoretical description of aggregate absorption (in terms of τ_s/π) (bottom). In the top solid curve represents spectra of the aqueous solution containing TC aggregates; dashed curve, spectra of a monomer solution prepared by dissolving TC dye in methanol. In the bottom solid curve represents the spectrum of an aggregate; dashed curve - spectrum of a monomer. Dimensionless parameter $\delta = \tau_s(\omega - \omega_{21})$ increases when the wavelength decreases.

were found above. In order to satisfy Eq. (39), the wave number k should be complex $k = k' + ik''$. Then using Eq. (39), we get for the real and imaginary part of k

$$k'\frac{c}{n_0} = \omega \mathrm{Re}\sqrt{1 + i\pi q\frac{W_a(\omega + p_1)}{1 - i\pi p_2 W_a(\omega + p_1)}} \tag{40}$$

and

$$k''\frac{c}{n_0} = \omega \mathrm{Im}\sqrt{1 + i\pi q\frac{W_a(\omega + p_1)}{1 - i\pi p_2 W_a(\omega + p_1)}}, \tag{41}$$

respectively. Fig. 7 shows the Frenkel EP dispersion calculated using Eqs. (40) and (41).

To give physical insight into the Frenkel EP dispersion, we shall calculate also the dispersion outside the resonance when $k'' \approx 0$. In that case Eq. (39) leads to the undamped polariton modes

$$k'\frac{c}{n_0} \approx \omega\sqrt{1 - \pi q \mathrm{Im}\frac{W_a(\omega + p_1)}{1 - i\pi p_2 W_a(\omega + p_1)}} \tag{42}$$

Taking spectrum $W_a(\omega)$ to be centered on $\omega = \omega_a$ and to have a finite width Γ, it is clear from the dispersion relation[30] that $W_a(\omega) \sim (i/\pi)/(\omega - \omega_a)$ for $|\omega - \omega_a| >> \Gamma$, and we get

$$k'\frac{c}{n_0} \approx \omega\sqrt{\frac{\omega - (\omega_a - p_1 - p_2) - q}{\omega - (\omega_a - p_1 - p_2)}} \tag{43}$$

Eq. (43) leads to two branches of the polariton dispersion shown in Fig. 7, namely, the lower branch for $\omega < \omega_a - p_1 - p_2$, and the upper branch for $\omega > \omega_a - p_1 - p_2$. For $\omega \to \omega_a - p_1 - p_2$ the wavenumber diverges, $k' \to \infty$. No solution of Eq. (43) exists for frequences between $\omega_a - p_1 - p_2$ and $(\omega_a - p_1 - p_2) + q$. In other words, there is a forbidden gap between $\omega_a - p_1 - p_2$ and $(\omega_a - p_1 - p_2) + q$ separating the lower and upper polariton branch. However, in the gap range more precise formulas, Eqs. (40) and (41), should be used, and the polariton dispersion shows the leaky part in the splitting range between two branches, Fig. 7.

From Eq. (43) we get for low frequencies, $\omega << \omega_a - p_1 - p_2$, a photon-like dispersion

$$\omega \simeq \frac{ck'}{n_0\sqrt{1 + q/(\omega_a - p_1 - p_2)}} \tag{44}$$

with a light velocity smaller than c/n_0.

From the above discussion, it is evident that parameter $q = \frac{4\pi}{\hbar}\eta N|\mathbf{D}_{12}|^2$ defines the separation between the lower and upper polariton branch. For the molecules of the same orientation ($\eta = 1$) that corresponds to experiment,[4] and $D_{12} \sim 10^{-17} CGSE$, $N = 10^{21}\ cm^{-3}$, one obtains the evaluation $q \simeq 6322\ cm^{-1}$. This value agrees with the measurements of Ref. 4. The position of the fluorescence

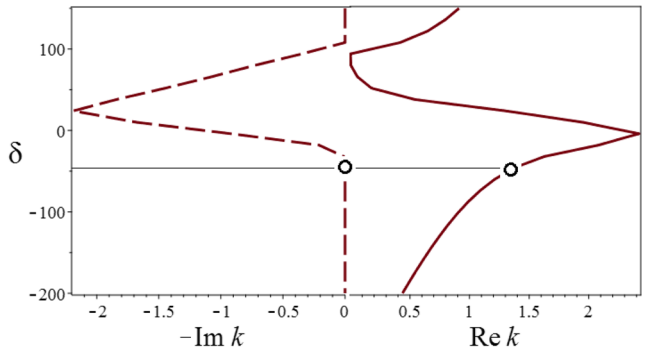

FIG. 7. Frenkel EP dispersion for real (solid line) and imaginary (dashed line) part of the wave number k calculated with Eqs. (40) and (41), respectively, when $q\tau_s = 84$. Other parameters are identical to those of the bottom of Fig. 5. k is in units of $c/(\omega_{21}n_0)$. Circles show the position of the fluorescence spectrum of a nanofiber.

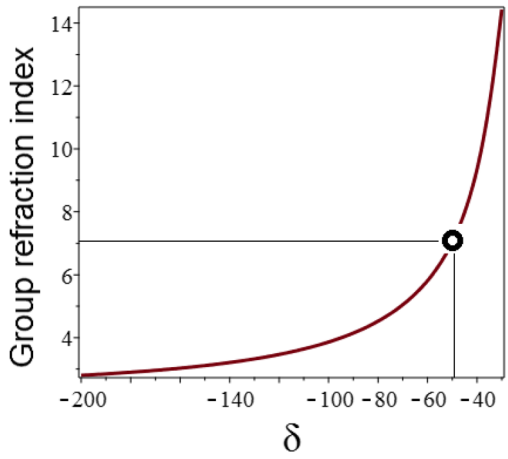

FIG. 8. Real part of the group refraction index n_g for $n_0 = 1.5$. Other parameters are identical to those of Figs. 5 and 7. Circle shows the position of the fluorescence spectrum of a nanofiber. Parameter $\delta = \tau_s(\omega - \omega_{21})$.

spectrum of a nanofiber that is in the range of ~ 2.5 eV is shown as circles in Fig. 7. One can see that it is located in the range where $\mathrm{Im}k \approx 0$, and it is out of the splitting range under discussion. That is why the fluorescence was amplified well in experiment.[4]

Fig. 8 shows the real part of the group refraction index $n_g(\omega) = n(\omega) + \omega dn(\omega)/d\omega$ as a function of frequency where $n(\omega) = (c/\omega)k(\omega)$ is the phase refraction index. The curve of Fig. 8 agrees with the experimental curve of Fig. 2a of Ref. 4. Both curves give the same value $\mathrm{Re}n_g \approx 7$ at the position of the fluorescence spectrum of a nanofiber (~ 2.5 eV).

V. CONCLUSION

In this work we have developed a mean-field electron-vibrational theory of Frenkel EPs in organic dye structures. Our consideration is based on the model of the interaction of strong shaped laser pulse with organic molecules, Refs. 6–8, extended to the dipole-dipole intermolecular interactions in the condensed matter. We show that such a generalization can describe both a red shift of the resonance frequency of isolated molecules, according to the CMLL mechanism,[9] and the wide variations of their spectra related to the aggregation of molecules into J- or H-aggregates. In particular case of weak radiation we recover the CES approximation.[10,29,30] We show that the experimental absorption spectra of H-aggregates (pinacyanol in aqueous solution at $20^{\circ}C$ and in aqueous solution with 7.5% v/v ethanol at room temperature) may be correctly described only if one takes both mechanisms into account. Our theory contains experimentally measured quantities that makes it closely related to experiment, and provides a possibility of generalization to a nonlinear regime. Indeed, the CMLL mechanism allows the most direct extension of approach, Refs. 6–8, to dipole-dipole intermolecular interactions in the condensed matter including the absence of vibrational equilibrium in electronic states (see Eq. (10)). In the case of wide variations of the molecular spectra related to the aggregation of molecules into J- or H-aggregates, extension to stronger radiation was made for the fast vibrational relaxation limit for J-aggregates (see Eq. (28) and Fig. 3). In essense, Eq. (28) generalizes the CES approximation to a nonlinear regime.

We have applied the theory to experiment on fraction of a millimeter propagation of Frenkel EPs in photoexcited organic nanofibers made of thiacyanine dye.[4] A good agreement between theory and experiment is obtained.

The theory can be also applied to plexcitonics[38] and the problems related to optics of exciton-plasmon nanomaterials.[39,40]

ACKNOWLEDGMENTS

I thank G. Rosenman and B. Apter who attracted my attention to Ref. 4.

APPENDIX

In the case of the Gaussian modulation of the electronic transition by the vibrations the absorption lineshape is given by[11,12,24,41]

$$F_a(\omega) = \frac{1}{\pi}\mathrm{Re}\int_0^\infty \exp[i(\omega - \omega_{21})t + g(t)]dt \tag{A1}$$

where

$$g(t) = -\int_0^t dt'(t - t')K(t') \tag{A2}$$

is the logarithm of the characteristic function of the spectrum of single-photon absorption after substraction of a term which is linear with respect to t and determines the first moment of the spectrum, $K(t)$ is the correlation function. Eq. (A1) can be used in general case when the "slow modulation" limit is not realized. Then the monomer spectrum is given by

$$W_a(\omega) = \frac{1}{\pi}\int_0^\infty \exp[i(\omega - \omega_{21})t + g(t)]dt \tag{A3}$$

For the exponential correlation function $K_s(t) = \sigma_{2s}\exp(-|t|/\tau_s)$, we get

$$g_s(t) = -\sigma_{2s}\tau_s^2[\exp(-t/\tau_s) + \frac{t}{\tau_s} - 1] \tag{A4}$$

that leads to Eq. (26) of Section II B.

[1] L. Gu, J. Livenery, G. Zhu, E. E. Narimanov, and M. A. Noginov, Applied Phys. Lett. **103**, 021104 (2013).
[2] M. J. Gentile, S. Nunez-Sánchez, and W. L. Barnes, Nano Letters **14**, 2339 (2014).
[3] T. U. Tumkur, J. K. Kitur, L. Gu, G. Zhu, and M. A. Noginov, ACS Photonics **2**, 622 (2015).
[4] K. Takazawa, J. Inoue, K. Mitsuishi, and T. Takamasu, Phys. Rev. Letters **105**, 067401 (2010).
[5] K. Takazawa, J. Inoue, K. Mitsuishi, and T. Kuroda, Advanced Functional Materials **23**, 839 (2013).
[6] B. D. Fainberg, J. Chem. Phys. **109**, 4523 (1998).
[7] B. D. Fainberg and V. Narbaev, J. Chem. Phys. **113**, 8113 (2000).
[8] B. D. Fainberg and V. Narbaev, J. Chem. Phys. **116**, 4530 (2002).
[9] M. V. Klein and T. E. Furtak, *Optics* (Wiley, New York, 1988).
[10] A. Eisfeld and J. S. Briggs, Chem. Phys. **324**, 376 (2006).
[11] B. D. Fainberg, in *Advances in Multiphoton Processes and Spectroscopy*, edited by S. H. Lin, A. A. Villaeys, and Y. Fujimura (World Scientific, Singapore, New Jersey, London, 2003), vol. 15, pp. 215–374.
[12] S. Mukamel, *Principles of Nonlinear Optical Spectroscopy* (Oxford University Press, New York, 1995).
[13] B. D. Fainberg, Opt. Spectrosc. **68**, 305 (1990) [Opt. Spektrosk. **68**, 525 (1990)].
[14] B. Fainberg, Phys. Rev. A **48**, 849 (1993).
[15] B. D. Fainberg, Chem. Phys. **148**, 33 (1990).
[16] A. S. Davydov, *Theory of Molecular Excitons* (Plenum, New York, 1971).
[17] S. Mukamel and D. Abramavicius, Chem. Rev. **104**, 2073 (2004).
[18] B. D. Fainberg and B. Levinsky, Adv. Phys. Chem. **2010**, 798419.
[19] B. D. Fainberg and G. Li, Applied Phys. Lett. **107**, 053302 (2015); Erratum **107**, 109902 (2015).
[20] M. Abramowitz and I. Stegun, *Handbook on Mathematical Functions* (Dover, New York, 1964).
[21] B. D. Fainberg, N. N. Rosanov, and N. A. Veretenov, Applied Phys. Lett. **110**, 203301 (2017).
[22] H. Haug and S. W. Koch, *Quantum theory of the optical and electronic properties of semiconductors* (World Scientific, Singapore, 2001).
[23] S. G. Rautian and I. I. Sobel'man, Soviet Physics Uspekhi **9**, 701 (1967) [Usp. Fiz. Nauk. **90**, 209–238 (1966)].
[24] B. D. Fainberg, Opt. Spectrosc. **58**, 323 (1985) [Opt. Spektrosk. **58**, 533 (1985)].
[25] K. Minoshima, M. Taiji, K. Misawa, and T. Kobayashi, Chem. Phys. Lett. **218**, 67 (1994).
[26] Y. Toyozawa, Progr. Theor. Phys. Suppl. **12**, 111 (1958).
[27] K. Takazawa, Y. Kitahama, Y. Kimura, and G. Kido, Nano Letters **5**, 1293 (2005).
[28] K. Takazawa, J. Phys. Chem. C **111**, 8671 (2007).
[29] A. Eisfeld and J. S. Briggs, Chem. Phys. **281**, 61 (2002).
[30] A. Eisfeld and J. S. Briggs, Phys. Rev. Lett. **96**, 113003 (2006).
[31] G. A. Baker, Jr. and P. Graves-Morris, *Padé Approximants* (Addison-Wesley Publishing Company, London, 1981).
[32] R. K. Saibatalov and B. D. Fainberg, Khim. Fizika (Chemical Physics) **6**, 163 (1987) (in Russian).
[33] V. A. Malyshev and P. Moreno, Phys. Rev. A **53**, 416 (1996).
[34] M. L. Horng, J. Gardecki, A. Papazyan, and M. Maroncelli, J. Phys. Chem. **99**, 17311 (1995).
[35] T. Joo, Y. Jia, J.-Y. Yu, M. J. Lang, and G. R. Fleming, J. Chem. Phys. **104**, 6089 (1996).
[36] B. D. Fainberg and D. Huppert, Adv. Chem. Phys. **107**, 191 (1999).
[37] S. H. Lin, Theor. Chim. Acta **10**, 301 (1968).

[38] N. J. Halas, S. Lal, W.-S. Chang, S. Link, and P. Nordlander, Chem. Rev. **111**, 3913 (2011).
[39] A. J. White, B. D. Fainberg, and M. Galperin, J. Phys. Chem. Lett. **3**, 2738 (2012).
[40] M. Sukharev and A. Nitzan, J. Phys.: Condens. Matter **29**, 443003 (2017).
[41] R. Kubo (Oliver Boyd, Edinburgh, 1962), p. 23.